

# Robust Trajectory Tracking Control of a Differentially Flat Overhead Crane Using Sliding Mode

Barnabás Finta<sup>1\*</sup>, Bálint Kiss<sup>1</sup>

<sup>1</sup> Department of Control Engineering and Information Technology, Faculty of Electrical Engineering and Informatics, Budapest University of Technology and Economics University, Műegyetem rkp. 3., H-1111 Budapest, Hungary

\* Corresponding author, e-mail: [finta@iit.bme.hu](mailto:finta@iit.bme.hu)

Received: 30 December 2022, Accepted: 06 September 2023, Published online: 19 January 2024

## Abstract

The control of overhead cranes is a benchmark problem, since it is an underactuated mechanism and its mathematical model is nonlinear. During operation the mass of the load is unknown, representing an uncertainty in the inertial parameters, which requires robustness of the controlled system. Our paper proposes a novel robust control method, that combines the differentially flat property of the dynamics with the robustness of the sliding mode control. The sliding surface is constructed to ensure the tracking of the configuration variables whose accelerations is calculated using the flatness property of the dynamic model. This formulation also allows achieving the matching conditions of the parameter uncertainties. Considering a simplified overhead crane model where the load motion is restricted in a vertical plane, two sliding surfaces are defined for the rope angle and rope length, since the cart position can be calculated from the previous two. The suggested control method is successfully validated in simulations as well as using a reduced-size overhead crane. For the real crane, the rope angle was estimated by utilizing the dynamical model, which uses the estimated cart acceleration.

## Keywords

crane control, flatness, sliding mode, robustness, sway estimation

## 1 Introduction

Overhead cranes assist the handling of heavy loads in many industrial activities at construction sites, in harbors, and in factories to name a few. Their widespread use justify largely the continuous attention of scientists in control theory since robust and time optimal automation of crane operations have considerable practical benefits in terms of efficiency and safety.

Overhead cranes, and other similar equipment using ropes, show ability for underdamped sway of the load. Since the motion of the suspended load in any horizontal direction requires that the force in the suspending rope have horizontal components such sway is always potentially generated if the load is displaced. Load sway can be further amplified by external disturbances such as wind or other environmental conditions.

Automatic control of cranes has a rich literature where the suggested methods aim to move the load quickly and without residual sway. A more comprehensive review of crane control methods can be found in [1] and [2].

Open-loop strategies exist to minimize load sway. The so-called input shaping filters out frequency components of the input signal that may excite the oscillation of the load [3, 4].

For closed-loop control, one may linearize the nonlinear dynamics and design linear controllers, such as serial compensators [5], LQG [6] or robust [7, 8] feedback laws. Controllers designed based on the linear approximation of the dynamics can only guarantee the stability of the closed-loop system in a neighborhood of the operating point. However, quick operations require large accelerations, which imply that the variables wander away from the operating point, where the linearized model remains valid.

Another family of controllers is suggested considering the nonlinear crane dynamics. One such approach is based on the differential flatness property [9, 10], where the load coordinates are shown to be the flat (or linearizing) outputs. The flatness property implies exact linearizability, a comfortable parameterization of available

system trajectories using the load coordinates, and the design of a stabilizing tracking controller. However, this model-based approach requires the knowledge of the inertia parameters including the load mass with adequate precision. To solve this problem adaptive algorithms can be used, that estimate the mass of the load, but during operation this can change very quickly when the load is hoisted from the ground or is being detached from the crane [11].

In this paper we propose a nonlinear control algorithm that combines the differential flatness property of the crane with sliding mode control to ensure robustness and provide increased disturbance rejection properties. The main contribution of the paper is to consider the effects of parameter uncertainties and external disturbances lumped into a single perturbation term, that satisfies the matching conditions [12] for the plant inputs. Then two sliding manifolds can be constructed along which the matched disturbances are exactly canceled. This effectively means that the flatness-based trajectory tracking controller achieves nominal performance even for the uncertain plant. The use of sliding mode control in crane systems with different techniques is also widely used [13, 14].

The remaining part of the paper is organized as follows. Since the proposed controller is model based section 2 derives the model of the overhead crane system using the Euler-Lagrange equations. This model is developed for the purposes of tracking a reference trajectory with the load and as such, some reasonable simplifications are made, which doesn't reduce the effectiveness of the developed control method in normal operating conditions. A more elaborate model for vibration control purposes is developed in [15]. Section 3 deals with the controller synthesis. First, in subsection 3.1 the exact linearization of the nominal system based on differential flatness is reviewed. Then the perturbed model is introduced in Section 3.2. Finally in Section 3.3 the full closed loop system is robustified utilizing sliding mode control. Section 4 contains the simulation results and Section 5 presents the measurements on a reduced-size crane setup in a laboratory setting.

## 2 Model of the crane system

The first step is to determine the dynamic equation of the plant to be controlled.

The setup is illustrated in Fig. 1. The load can move in a vertical plane. The configuration variables of the system are the cart position  $R$ , the rope length  $L$ , and the rope angle  $\theta$ . The parameters are the cart and load masses  $M$  and  $m$  respectively, the rotational inertia  $J$ , and radius  $\rho$  of the

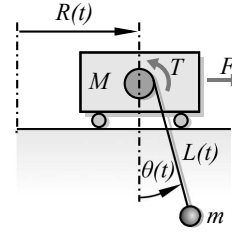


Fig. 1 Variables and parameters of the planar overhead crane

winch. The cable is assumed massless, since the mass of the load is significantly greater than that of the cable itself. To obtain the mathematical model for the crane one might use the Euler-Lagrange equations in the form:

$$\frac{d}{dt} \left( \frac{\partial \mathcal{L}}{\partial \dot{\mathbf{q}}} \right) - \frac{\partial \mathcal{L}}{\partial \mathbf{q}} = \boldsymbol{\tau}, \quad (1)$$

where  $\mathbf{q} = [R \ L \ \theta]^T$  and the Lagrangian reads  $\mathcal{L}(\mathbf{q}, \dot{\mathbf{q}}) = E(\mathbf{q}, \dot{\mathbf{q}}) - P(\mathbf{q})$  so that that the kinetic energy and the potential energy is given with the expressions:

$$E(\mathbf{q}, \dot{\mathbf{q}}) = \frac{1}{2} M \times \mathbf{v}_{cart}^2 + \frac{1}{2} m \times \mathbf{v}_{load}^2 + \frac{1}{2} J \left( \frac{\dot{L}}{\rho} \right)^2. \quad (2)$$

$$P(\mathbf{q}) = -mgL \cos \theta$$

The load velocity is expressed as function of  $\mathbf{q}$  and  $\dot{\mathbf{q}}$ :

$$\mathbf{v}_{load} = \begin{bmatrix} \dot{x}_m \\ \dot{z}_m \end{bmatrix} = \begin{bmatrix} \dot{R} + \dot{L} \sin \theta + L \dot{\theta} \cos \theta \\ \dot{L} \cos \theta - L \dot{\theta} \sin \theta \end{bmatrix}. \quad (3)$$

The velocity of the cart is trivially  $\mathbf{v}_{cart} = \dot{R}$ . The resulting crane dynamics has the form:

$$\mathbf{H}(\mathbf{q}) \ddot{\mathbf{q}} + \mathbf{h}(\mathbf{q}, \dot{\mathbf{q}}) = \boldsymbol{\tau}, \quad (4)$$

where:

$$\mathbf{H}(\mathbf{q}) = \begin{bmatrix} M + m & m \sin \theta & mL \cos \theta \\ m \sin \theta & m + J/\rho^2 & 0 \\ mL \cos \theta & 0 & mL^2 \end{bmatrix}, \quad (5)$$

$$\mathbf{h}(\mathbf{q}, \dot{\mathbf{q}}) = \begin{bmatrix} 2m\dot{L}\dot{\theta} \cos \theta - mL\dot{\theta}^2 \sin \theta \\ -mL\dot{\theta}^2 - mg \cos \theta \\ mL(2\dot{L}\dot{\theta} + g \sin \theta) \end{bmatrix}, \quad (6)$$

$$\boldsymbol{\tau}(\mathbf{t}) = \begin{bmatrix} F \\ -T \\ 0 \end{bmatrix}. \quad (7)$$

For later use, let us remark that the model is invariant with respect to  $R$  and  $\dot{R}$ . Let us also note that the model

does not include (nonlinear) friction phenomena of the cart and the winch as these effects are later considered as external disturbances.

The model equations are valid if the rope tension is positive (the load is not pushed using the rope) and the sway angle stays in the  $(-90^\circ, +90^\circ)$  interval (where  $\cos \theta > 0$ ). Both conditions are fulfilled for realistic crane operations, no small angle approximations are employed.

### 3 Controller synthesis

This section walks over the necessary steps of designing a novel robust controller for the two dimensional (2D) overhead crane system using differential flatness based exact linearization and sliding mode control.

#### 3.1 Exact linearization based on differential flatness

The 2D overhead crane system's model belongs to the class of differentially flat systems. Roughly speaking a system is differentially flat, if one can find a set of so-called flat outputs (that are equal in number to the inputs), such that all the states and inputs of the system can be expressed by the flat outputs and some finite number of their derivatives. Moreover, if a system possesses the flatness property, then it is linearizable by dynamic state feedback and a change of coordinates.

The method presented here follows the developments in [16], and also referenced in [10]. It is shown that exact linearization is only possible via dynamic feedback [17].

It can be shown that the load's coordinates, denoted by  $x_m$  and  $z_m$ , are the flat outputs of the system. To obtain the expressions of the model variables  $(R, L, \theta, \dot{R}, \dot{L}, \dot{\theta})$  using  $(x_m, z_m)$  and their derivatives, let us consider the free-body diagram of the load, depicted in Fig. 2.

The load's equations of motion read

$$\begin{aligned} m\ddot{x}_m &= -F_L \sin \theta \\ m\ddot{z}_m &= -F_L \cos \theta + mg \end{aligned} \quad (8)$$

Using these equations and elementary geometry one gets:

$$\begin{aligned} \theta &= \operatorname{atan} \left( \frac{\ddot{x}_m}{\ddot{z}_m - g} \right) \quad L = -z_m \frac{\sqrt{(\ddot{z}_m - g)^2 + \ddot{x}_m}}{\ddot{z}_m - g} \\ R &= x_m - \rho - z_m \frac{\dot{x}_m}{\ddot{z}_m - g} \end{aligned} \quad (9)$$

The input variables  $F$  and  $T$  can be obtained as functions of  $x_m, z_m$  and their time derivatives using Eq. (4). To construct the dynamic feedback we use the steps presented in [10]. The variables  $\zeta_1, \zeta_2$  are introduced as:

$$\zeta_1 = F_L/m \quad \zeta_2 = \dot{F}_L/m = \dot{\zeta}_1. \quad (10)$$

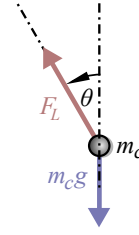


Fig. 2 The forces acting on the load

They correspond to the states of the dynamic state feedback so that the closed-loop linear system is linear and has the form:

$$x_m^{(4)} = y_1^{(4)} = v_1 \quad z_m^{(4)} = y_2^{(4)} = v_2. \quad (11)$$

The linearizing feedback structure is presented in Fig. 3. Let us introduce the standard notation of  $S_\theta = \sin \theta$  and  $C_\theta = \cos \theta$ .

Block A realizes the expression:

$$\begin{bmatrix} \dot{\zeta}_2 \\ \dot{\theta} \end{bmatrix} = \begin{bmatrix} -S_\theta & -\zeta_1 C_\theta \\ -C_\theta & \zeta_1 S_\theta \end{bmatrix}^{-1} \begin{bmatrix} v_1 - \zeta_1 \theta^2 S_\theta - 2\zeta_2 \dot{C}_\theta \\ v_2 - \zeta_1 \theta^2 C_\theta - 2\zeta_2 \dot{S}_\theta \end{bmatrix}. \quad (12)$$

Block B contains:

$$\begin{bmatrix} \ddot{R} \\ \ddot{L} \end{bmatrix} = F_1^{-1} \left( F_2 \begin{bmatrix} \zeta_1 \\ \dot{\theta} \end{bmatrix} + \begin{bmatrix} L\dot{\theta}^2 S_\theta - 2L\dot{\theta} \\ g + L\dot{\theta}^2 C_\theta + 2L\dot{\theta}S_\theta \end{bmatrix} \right), \quad (13)$$

where:

$$F_1 = \begin{bmatrix} 1 & S_\theta \\ 0 & C_\theta \end{bmatrix}, \quad F_2 = \begin{bmatrix} -S_\theta & -LC_\theta \\ -C_\theta & LS_\theta \end{bmatrix}, \quad (14)$$

and Block C contains Eq. (4), namely the dynamic model of the crane.

Let us emphasize that all inertia parameters are concentrated in Block C. The inputs of this block, denoted by  $[\ddot{R}_d, \ddot{L}_d, \ddot{\theta}_d]^T$ , can be thought of as the desired accelerations of the configuration variables for which the inputs are calculated.

Thus exact linearization of the crane system is achieved with the feedback structure shown in Fig. 3. This is achieved by dynamic feedback. It can be shown

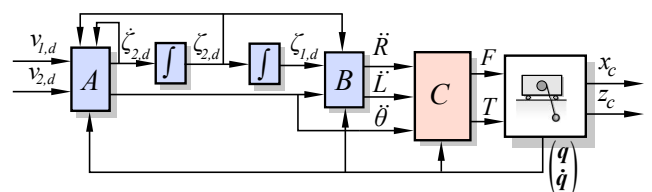


Fig. 3 The feedback structure of exact linearization resulting Eq. (11) in closed-loop

that no exact linearization can be achieved with less than two states in the feedback. Thus the closed loop system becomes two decoupled chains of integrators as in Eq. (11).

Eq. (11) allows the design of an additional tracking controller for sufficiently smooth load reference trajectory  $x_r(t)$ ,  $z_r(t)$ , ensuring the exponential decay of the tracking errors defined as  $e_x = x_r - x_m$  and  $e_z = z_r - z_m$ . For, it is enough to set the linear differential equations for the tracking errors:

$$e_x^{(4)} + \sum_{i=0}^3 \lambda_{x,i} e_x^{(i)} = 0 \quad e_z^{(4)} + \sum_{i=0}^3 \lambda_{z,i} e_z^{(i)} = 0, \quad (15)$$

from which the  $v_1, v_2$  can be expressed as:

$$v_1 = x_r^{(4)} + \sum_{i=0}^3 \lambda_{x,i} e_x^{(i)} \quad v_2 = z_r^{(4)} + \sum_{i=0}^3 \lambda_{z,i} e_z^{(i)}. \quad (16)$$

Using Eq. (11). The scalar coefficients  $\lambda_{x,i}, \lambda_{z,i}$  are design parameters used to set the decay rate of the error so that all roots of the characteristic equations of Eq. (15) are in the stable region of the complex plane. The derivatives of the load coordinates in Eq. (16) can be calculated using  $q, \dot{q}, \zeta_1, \zeta_2$ , hence no numerical differentiation is required. Fig. 4. depicts the closed loop after applying the tracking controller so that  $\bar{x}_r = [x_r, \dot{x}_r, \dots, x_r^{(4)}]^T$  and  $\bar{z}_r = [z_r, \dot{z}_r, \dots, z_r^{(4)}]^T$ .

The reference path  $x_r$  and  $z_r$  needs to be constructed such that their time derivatives up to the fourth degree exists. Typically, idle-to-idle trajectories are constructed with polynomial time functions.

The feedback constructed so far considered only the model with nominal inertia parameters. The following subsection deals with the case where the parameters of the crane differ from the nominal ones and the system is subject to disturbances such as non-modeled friction forces.

### 3.2 The perturbed model

Here we analyze the effect of uncertain inertia parameters and external disturbances on the crane dynamics. Uncertain inertia parameters are the mass of the cart and load. Nonlinear friction forces can be considered as external disturbances. The following assumption is made.

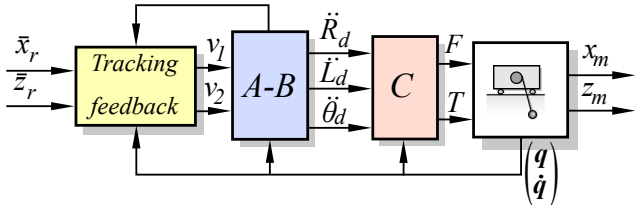


Fig. 4 Closed-loop interconnections with the tracking controller

The external disturbances  $d$  are modelled as:

$$H(q)\ddot{q} + h(q, \dot{q}) = \tau + d, \quad (17)$$

such that  $d = [d_1, d_2, 0]^T$ , hence we assume that the external disturbance only affects the acceleration of the cart and the acceleration of the rope length (e.g., in the form of friction), no disturbance acts directly on the rope angle.

The assumption defines the types of disturbances for which the closed loop can be made invariant, since later in this subsection it is shown that these satisfy the matching conditions [12]. Based on the form of the disturbance  $d$  in Eq. (17), the last component of Eq. (4) reads:

$$mL \cos \theta \ddot{R} + mL \ddot{\theta} + mL(2\dot{L}\dot{\theta} + g \sin \theta) = 0, \quad (18)$$

hence a simplification by  $m$  is possible ( $m > 0$  holds true for any load):

$$L \cos \theta \ddot{R} + L \ddot{\theta} + L(2\dot{L}\dot{\theta} + g \sin \theta) = 0. \quad (19)$$

Eq. (19) contains no inertia parameter or forces/torques so one can express  $\ddot{R}$  as:

$$\ddot{R} = \frac{-1}{L \cos \theta} (L \ddot{\theta} + L(2\dot{L}\dot{\theta} + g \sin \theta)). \quad (20)$$

Thanks to the invariance of the model with respect to  $R$  and  $\ddot{R}$ , a reduced model can be obtained by substituting Eq. (20) back into Eq. (4). For the reduced configuration vector  $\tilde{q} = [L, \theta]^T$  the reduced model reads:

$$\tilde{H}(\tilde{q})\ddot{\tilde{q}} + \tilde{h}(\tilde{q}, \dot{\tilde{q}}) = \tilde{A} + \tilde{d} = \begin{bmatrix} F \\ -T \end{bmatrix} + \begin{bmatrix} d_1 \\ d_2 \end{bmatrix}, \quad (21)$$

where:

$$\tilde{H} = \begin{bmatrix} mS_\theta & LmC_\theta - L(M+m)/C_\theta \\ (m\rho^2 + J)/\rho^2 & -Lms_\theta/C_\theta \end{bmatrix}, \quad (22)$$

$$\tilde{h} = \begin{bmatrix} \frac{gmS_\theta - 2(M + mS_\theta^2)\dot{L}\dot{\theta}}{C_\theta} \\ \frac{-MgS_\theta - mL\dot{\theta}^2 S_\theta C_\theta}{C_\theta} \\ \frac{m(LC_\theta\dot{\theta}^2 + 2\dot{L}\dot{\theta}S_\theta + g)}{C_\theta} \end{bmatrix}. \quad (23)$$

Note that in the matrix of Eq. (22) some elements are divided by  $C_\theta$ , meaning that the effects of uncertainties are magnified as the rope angle approaches  $\pm 90^\circ$ , which is a singularity of the model.

Let us denote by  $\hat{\mathbf{H}}$  and  $\hat{\mathbf{h}}$  the matrices  $\tilde{\mathbf{H}}$  and  $\tilde{\mathbf{h}}$  with components calculated with the nominal inertia parameter values. The linearizing feedback law for the nominal system without disturbance can be calculated as

$$\tilde{\tau} = \hat{\mathbf{H}}(\tilde{\mathbf{q}})\tilde{\mathbf{a}} + \hat{\mathbf{h}}(\tilde{\mathbf{q}}, \dot{\tilde{\mathbf{q}}}), \quad (24)$$

where  $\tilde{\mathbf{a}} = [a_L, a_\theta]^T$  denotes the accelerations. The parameter uncertainties modify the nominal components as:

$$\begin{aligned} \hat{\mathbf{H}} - \Delta\tilde{\mathbf{H}} &= \tilde{\mathbf{H}} \\ \hat{\mathbf{h}} - \Delta\tilde{\mathbf{h}} &= \tilde{\mathbf{h}} \end{aligned} \quad (25)$$

Applying Eq. (24) to the reduced model of Eq. (21), the closed-loop dynamics read:

$$\ddot{\tilde{\mathbf{q}}} = \tilde{\mathbf{a}} + \tilde{\mathbf{H}}^{-1}\Delta\tilde{\mathbf{H}}\tilde{\mathbf{a}} + \tilde{\mathbf{H}}^{-1}(\Delta\tilde{\mathbf{h}} + \tilde{\mathbf{d}}). \quad (26)$$

Next, we show that the uncertainties satisfy the so-called matching conditions.

For the sake of completeness, let us summarize the concept of matching conditions [14]. Consider an uncertain nonlinear state equation in the form:

$$\dot{\mathbf{x}} = \mathbf{f}(\mathbf{x}) + \Delta\mathbf{f}(\mathbf{x}) + \mathbf{G}(\mathbf{x})\mathbf{u} + \Delta\mathbf{G}(\mathbf{x})\mathbf{u}, \quad (27)$$

This system is said to satisfy the matching conditions if the uncertain terms can be factorized as follows:

$$\begin{aligned} \Delta\mathbf{f}(\mathbf{x}) &= \mathbf{G}(\mathbf{x})\Delta\bar{\mathbf{f}}(\mathbf{x}) \\ \Delta\mathbf{G}(\mathbf{x}) &= \mathbf{G}(\mathbf{x})\Delta\bar{\mathbf{G}}(\mathbf{x}) \end{aligned} \quad (28)$$

and if there exists positive constant such that:

$$\|\Delta\bar{\mathbf{G}}\| \leq 1 - \varepsilon. \quad (29)$$

The uncertainties satisfying the matching conditions are called matched uncertainties.

If the matching conditions are satisfied, then Eq. (27) can be rearranged into the form:

$$\dot{\mathbf{x}} = \mathbf{f}(\mathbf{x}) + \mathbf{G}(\mathbf{x})(\mathbf{u} + \Delta(\mathbf{x}, \mathbf{u})), \quad (30)$$

where  $\Delta(\mathbf{x}, \mathbf{u})$  is a uniformly bounded unknown function that lumps together uncertainties and external disturbances. To ensure robustness against  $\Delta(\mathbf{x}, \mathbf{u})$  the upper bound of its norm  $|\Delta(\mathbf{x}, \mathbf{u})|$  needs to be known.

Let us now show that the crane dynamics satisfy the matching conditions. Considering the dynamics given by Eq. (26), the corresponding state equation reads:

$$\frac{d}{dt} \begin{bmatrix} \tilde{\mathbf{q}} \\ \dot{\tilde{\mathbf{q}}} \end{bmatrix} = \begin{bmatrix} \dot{\tilde{\mathbf{q}}} \\ \tilde{\mathbf{H}}^{-1}(\Delta\tilde{\mathbf{h}} + \tilde{\mathbf{d}}) \end{bmatrix} + \begin{bmatrix} \mathbf{0} \\ \mathbf{I} + \tilde{\mathbf{H}}^{-1}\Delta\tilde{\mathbf{H}} \end{bmatrix} \tilde{\mathbf{a}}. \quad (31)$$

Let us introduce the notations:

$$\begin{aligned} \mathbf{f}(\mathbf{x}) &= \begin{bmatrix} \dot{\tilde{\mathbf{q}}} \\ \mathbf{0} \end{bmatrix}, \quad \mathbf{G}(\mathbf{x}) = \begin{bmatrix} \mathbf{0} \\ \mathbf{I} \end{bmatrix} \\ \Delta\mathbf{f}(\mathbf{x}) &= \begin{bmatrix} \mathbf{0} \\ \tilde{\mathbf{H}}^{-1}(\Delta\tilde{\mathbf{h}} + \tilde{\mathbf{d}}) \end{bmatrix}, \quad \Delta\mathbf{G}(\mathbf{x}) = \begin{bmatrix} \mathbf{0} \\ \tilde{\mathbf{H}}^{-1}\Delta\tilde{\mathbf{H}} \end{bmatrix}, \\ \Delta\bar{\mathbf{f}}(\mathbf{x}) &= \begin{bmatrix} \mathbf{0} \\ \tilde{\mathbf{H}}^{-1}(\Delta\tilde{\mathbf{h}} + \tilde{\mathbf{d}}) \end{bmatrix}, \quad \Delta\bar{\mathbf{G}}(\mathbf{x}) = \begin{bmatrix} \mathbf{0} \\ \tilde{\mathbf{H}}^{-1}\Delta\tilde{\mathbf{H}} \end{bmatrix} \end{aligned} \quad (32)$$

The matched uncertainties act along the control distribution spanned by the columns of  $\mathbf{G}(\mathbf{x})$ , so matched uncertainties generate motion directions in the state space which can be directly eliminated by the control action.

For the crane system we define  $\mathbf{u}$  and  $\Delta(\mathbf{x}, \mathbf{u})$  as:

$$\Delta(\mathbf{x}, \mathbf{u}) = \begin{bmatrix} \Delta_1 \\ \Delta_2 \end{bmatrix}, \quad \mathbf{u} = \begin{bmatrix} F \\ -T \end{bmatrix}. \quad (33)$$

### 3.3 Robustifying the closed loop system

The aim is to introduce a new component in the feedback loop of Fig. 4 which ensures robustness against the matched uncertainties.

In the differential flatness-based control of Fig. 4 Block B calculates the term  $\ddot{\mathbf{q}}_d = [\ddot{R}_d, \ddot{L}_d, \ddot{\theta}_d]^T$ , which contains the desired acceleration for the rope length and the rope's angle.

Let us remark first that the compatible time functions for  $L_d, \dot{L}_d, \theta_d, \dot{\theta}_d$  can be calculated by integration as:

$$\begin{aligned} \dot{L}_{ref} &= \int \ddot{L}_d dt, \quad L_{ref} = \int \dot{L}_{ref} dt, \\ \dot{\theta}_{ref} &= \int \ddot{\theta}_d dt, \quad \theta_{ref} = \int \dot{\theta}_{ref} dt. \end{aligned} \quad (34)$$

Now it is possible to define a tracking error in the reduced configuration variables:

$$\tilde{\mathbf{q}}_e := \begin{bmatrix} L_{ref} - L \\ \theta_{ref} - \theta \end{bmatrix} = \tilde{\mathbf{q}}_{ref} - \tilde{\mathbf{q}}. \quad (35)$$

A sliding mode controller is constructed to eliminate  $\tilde{\mathbf{q}}_e$  so that the sliding surface is defined as:

$$\mathbf{s} = \dot{\tilde{\mathbf{q}}}_e + \Lambda\tilde{\mathbf{q}}_e, \quad (36)$$

The initial values of the integrators after the desired accelerations can be set as the initial values of the system, this way we start on the sliding surface, since the errors would be zero. A corresponding Lyapunov function is:

$$V(s) = \frac{1}{2} |s|^2, \quad (37)$$

whose time derivative along the trajectories of the perturbed subsystem is:

$$\dot{V}(s) = \frac{\partial V(s)}{\partial s} \times \dot{s} = s^T \dot{s} \leq -\eta |s|. \quad (38)$$

The time derivative of the sliding variable is thus:

$$\dot{s} = \ddot{q}_d - \ddot{a} - \left( \tilde{H}^{-1} \Delta \tilde{H} \ddot{a} + \tilde{H}^{-1} (\Delta \tilde{h} + \ddot{a}) \right) + \Lambda \dot{q}_e, \quad (39)$$

Now we need to choose  $\ddot{a}$  such that Eq. (38) holds. For that we use the following control signal:

$$\ddot{a} = \ddot{q}_d + \Lambda \dot{q}_e + K \times \text{sign}(s), \quad (40)$$

where  $\Lambda = \text{diag}(\lambda_L, \lambda_\theta)$ ,  $K = \text{diag}(K_L, K_\theta)$  and  $\lambda_L, \lambda_\theta, K_L, K_\theta > 0$  are constants that the designer needs to choose.

If we choose the gain  $K$  such that:

$$K > \left| \tilde{H}^{-1} \Delta \tilde{H} a + \tilde{H}^{-1} (\Delta \tilde{h} + \ddot{a}) \right| + \eta, \quad (41)$$

then Eq. (38) holds, meaning that the sliding surface is reached. The system becomes invariant to matched perturbations and the tracking errors decay exponentially, guaranteeing robust stability and performance. If the inequality (Eq. (38)) holds globally, then the sliding surface is reached from the whole state space. Thus, the robust control law  $\tau$  can be written as:

$$\tau = \hat{H}(q) \begin{bmatrix} a_R \\ a_L \\ a_\theta \end{bmatrix} + \hat{h}(q, \dot{q}), \quad (42)$$

where the variable  $a$  with subscript  $R, L, \theta$  denotes that it is the signal for the virtual acceleration inputs. The term  $a_R$  is calculated similarly to Eq. (20), where  $\ddot{R}, \ddot{\theta}$  are replaced with  $a_R, a_\theta$ .

To sum up, the robustified controller structure is the differential flatness based exact linearization depicted in Fig. 5, with the additional sliding mode controller. For this figure we used the shorthand notation of:

$$\begin{aligned} L_{SW} &= \lambda_L \dot{L}_e + K_L \times \text{sign}(s_L) \\ \theta_{SW} &= \lambda_\theta \dot{\theta}_e + K_\theta \times \text{sign}(s_\theta) \end{aligned} \quad (43)$$

The reference signals for the SMC are the integrals of the desired accelerations in the configuration variables computed by the Blocks A and B. The tracking controller

is left unchanged compared to Fig. 4. The final control structure is depicted in Fig. 5, where the block  $C$  is substituted by the block  $\tilde{C}$ , to show that it now performs the calculations of Eq. (42), instead of Eq. (4).

This structure ensures the satisfaction of the matching conditions. If instead the robustifying sliding mode signal is inserted into the tracking block, then one can show the opposite. The matching condition property is ruined by the integrators in the  $A$ - $B$  block of Fig. 5, which are necessary for exact linearization.

#### 4 Validation using simulation

This section is dedicated to the validation of the designed controller using simulations. Both the original exact linearization based controller (abbreviated as NORC after 'non-robust controller') and the robustified version with the sliding mode extension (abbreviated as SMC) are simulated to compare the results. The simulations are carried out using Matlab and Simulink [18].

The nominal plant has parameter values  $M = 0.3$  kg,  $m = 0.2$  kg,  $\rho = 0.03$  m,  $J = 0.001$  kg/m<sup>2</sup>. The tracking controller is synthesized such that the characteristic polynomial of the tracking error differential Eq. (15) has all four of its roots at  $1/T, T > 0$ , which results in:

$$\lambda_3 = \frac{3}{T}, \quad \lambda_2 = \frac{6}{T^2}, \quad \lambda_1 = \frac{3}{T^3}, \quad \lambda_0 = \frac{1}{T^4}. \quad (44)$$

The time constant  $T$  was chosen as 0.2 seconds. The values of  $K_L$  and  $K_\theta$  are both 10 and  $\lambda_L, \lambda_\theta$  are both 5. These can be further tuned to improve the controller.

A simple, polynomial, idle-to-idle trajectory was planned. Simulation runs are executed so that the load's mass is increased to four times its nominal value  $m = 0.8$  kg. Fig. 6 depicts the simulation results. Significant differences can be observed between the performances of the two controllers, the SMC achieves the same performance as with the nominal parameter values, while NORC could not achieve exponential decay of tracking errors.

Fig. 7 shows the control effort produced by the two controllers in case of perturbed parameters. It is clear that the

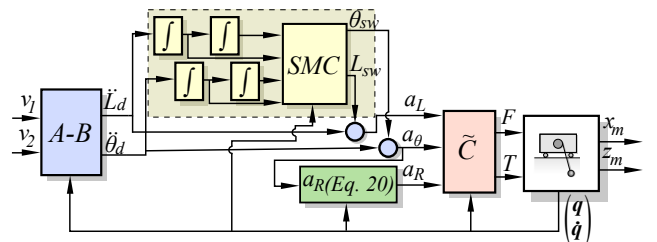


Fig. 5 The block diagram of the robustified closed loop system

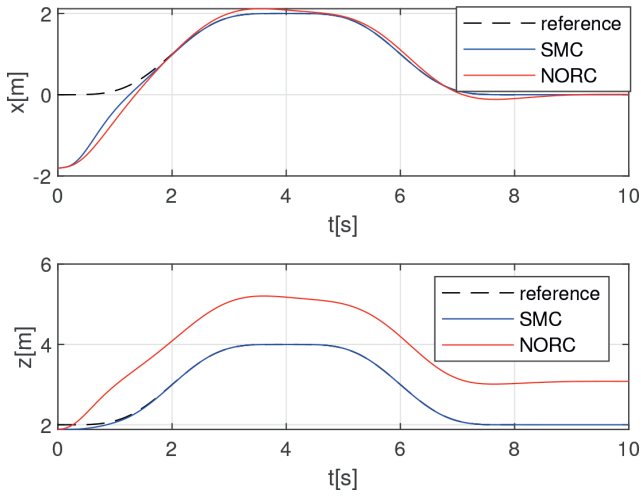


Fig. 6 Load coordinates for a system with perturbed parameter values and initial error in the horizontal direction

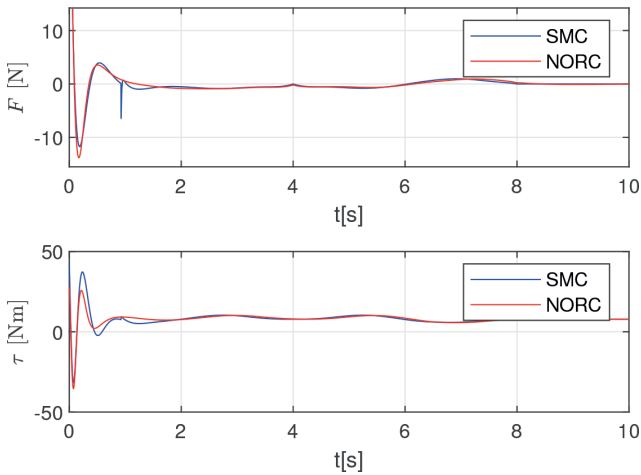


Fig. 7 Control signals for a system with perturbed parameter values

cost of better trajectory tracking is higher control effort, which is needed to attenuate the effects of uncertainties and disturbances. The spike in the force actuation may be caused by the reaching of the sliding surface.

### 5 Validation on a reduced-size crane setup

To test the controller, experiments were performed on a real, reduced-size 2D overhead crane setup in the laboratory of our department. This model, depicted in Fig. 8, is built upon the AMIRA inverted pendulum platform, the pendulum part is replaced with a winch mechanism.

There are incremental encoders measuring the displacement  $R(t)$  and the rope length  $L(t)$ . The rope angle  $\theta(t)$  is also measured by an incremental encoder, however these measurements were not used in the feedback. Instead, the rope angle was estimated by calculating the rope angle's second derivative:

$$\ddot{\theta}_{est} = -\frac{1}{L}(\ddot{R} \cos \theta_{est} + 2\dot{L}\dot{\theta}_{est} + g \sin \theta_{est}), \quad (45)$$

which is a rearrangement of Eq. (20). The *est* in the subscript expresses that the value is computed using Eq. (45) the derivatives  $\dot{R}(t)$ ,  $\dot{L}(t)$ ,  $\ddot{R}(t)$  are obtained by discrete differentiation of the corresponding measurement values. The output of the angle acceleration estimator Eq. (45) is integrated twice, the results  $\theta_{est}$ ,  $\dot{\theta}_{est}$  are fed back to the estimator, their initial values are zero, since the system starts from a resting position. The control system is operated by Quarc, which makes possible to run Simulink diagrams in real-time using Windows operating system. The sampling time was chosen as  $T_s = 1$  ms.

Fig. 9 shows the  $x$  and  $z$  load coordinates calculated with the rope angle measurement. It is clear that the sliding mode controller improved the trajectory tracking performance. The main source of uncertainty was friction, which was robustly compensated by SMC.

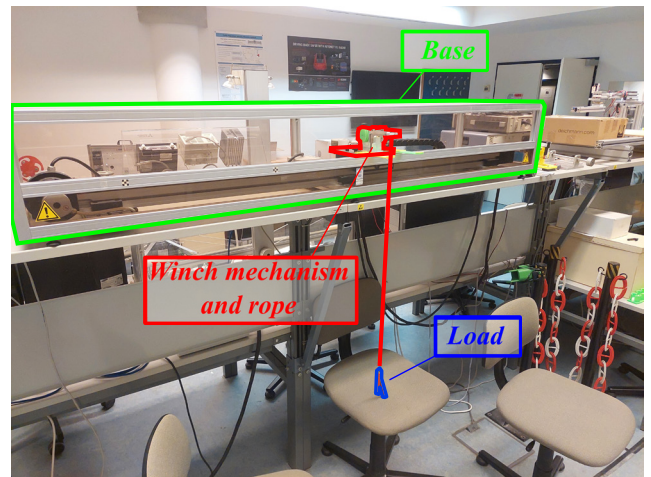


Fig. 8 The measurement setup in the laboratory

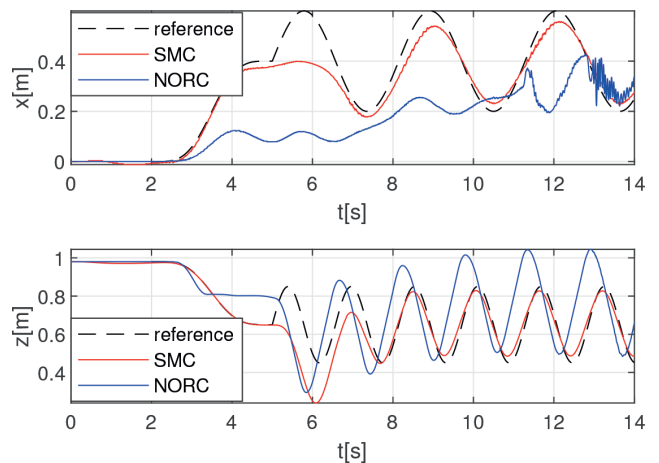


Fig. 9 Load coordinates calculated with the measured rope angle

In Fig. 10 the load's trajectory is drawn in the Euclidean coordinates to compare it to the reference shape. This also illustrates well the increased robustness of the tracking performance.

The controller effort is depicted in Fig. 11. The robust variant results in more chattering due to the higher gains of sliding mode control. For SMC, instead of the *sign* function the saturation function was applied, that generally results in less chattering, but it was not completely eliminated in this case.

Note that the aim here was to compare the robustified controller's behavior to the classical one. Likely these results can be significantly improved with more careful tuning of the controllers and taking into consideration the dynamics of the actuators. Also during the experiment a rather strict saturation term was inserted after the controllers output before the signal could appear at the actuators for safety reasons, removing this effect likely improves performance as well. Also, another possibility is to use more advanced differentiators to obtain  $\dot{R}(t)$ ,  $\dot{L}(t)$ ,  $\ddot{R}(t)$  (e.g., ones that use sliding modes), here only simple numeric backward differentiation was applied with some filtering to reduce noise, which also introduces phase lag.

## 6 Conclusion

The paper presented a sliding mode control based robust method for the trajectory tracking of a crane. The nominal control law is a dynamic exact linearizing feedback. This is augmented with the SMC by considering the desired accelerations in the configuration variables as virtual inputs. These accelerations are computed by the endogenous feedback. Two sliding surface corresponding to the rope length  $L$  and rope angle  $\theta$  are used to achieve invariance to the matched perturbations.

## References

- [1] Hyla, P. "The crane control systems: A survey", In: 2012 17th International Conference on Methods & Models in Automation & Robotics (MMAR), Miedzyzdroje, Poland, 2012, pp. 505–509. ISBN 9781467321242  
<https://doi.org/10.1109/mmar.2012.6347867>
- [2] Ramli, L., Mohamed, Z., Abdullahi, A. M., Jaafar, H. I., Lazim, I. M. "Control strategies for crane systems: A comprehensive review", Mechanical Systems and Signal Processing, 95, pp. 1–23, 2017.  
<https://doi.org/10.1016/j.ymssp.2017.03.015>
- [3] Garrido, S., Abderrahim, M., Gimenez, A., Diez, R., Balaguer, C. "Anti-swinging input shaping control of an automatic construction crane", IEEE Transactions on Automation Science and Engineering, 5(3), pp. 549–557, 2008.  
<https://doi.org/10.1109/tase.2007.909631>
- [4] Maghsoudi, M., Ramli, L., Sudin, S., Mohamed, Z., Husain, A., Wahid, H. "Improved unity magnitude input shaping scheme for sway control of an underactuated 3d overhead crane with hoisting", Mechanical systems and signal processing, 123, pp. 466–482, 2019.  
<https://doi.org/10.1016/j.ymssp.2018.12.056>
- [5] Lee, H. H. "Modeling and Control of a Three Dimensional Overhead Crane", Journal of Dynamic Systems, Measurement and Control, 120(4), pp. 471–476, 1998.  
<https://doi.org/10.1115/1.2801488>
- [6] Larsson, P. O., Braun, R. "Construction and control of an educational lab process-the gantry crane", In: Proceedings Reglermöte 2008, Luleå, Sweden, 2008, pp. 59–65. [online] Available at: [https://www.researchgate.net/publication/242293561\\_Construction\\_and\\_Control\\_of\\_an\\_Educational\\_Lab\\_Process\\_-\\_The\\_Gantry\\_Crane](https://www.researchgate.net/publication/242293561_Construction_and_Control_of_an_Educational_Lab_Process_-_The_Gantry_Crane) [Accessed: 26 June 2023]

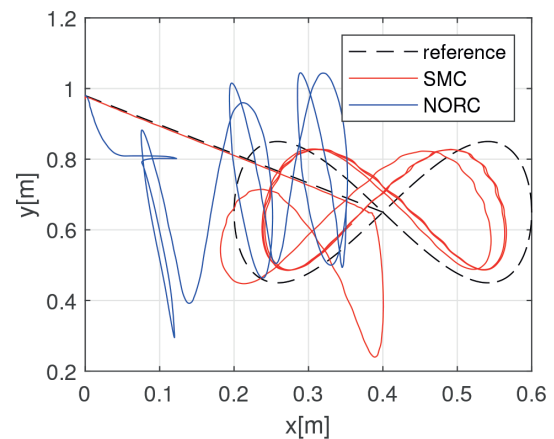


Fig. 10 Load coordinates in x-z calculated with the measured rope angle

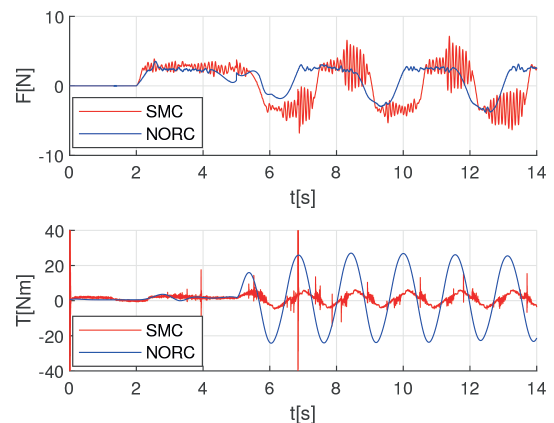


Fig. 11 Control signals during the measurement

Simulations show that the effect of external disturbances are greatly attenuated by the proposed control law, compared to the nominal control only, without SMC. Laboratory measurements were also performed, that also validated the control design.

- [7] Hilhorst, G., Pipeleers, G., Michiels, W., Oliveira, R. C., Peres, P. L., Swevers, J. "Fixed order linear parameter-varying feedback control of a lab-scale overhead crane", *IEEE Transactions on Control Systems Technology*, 24(5), pp. 1899–1907, 2016. <https://doi.org/10.1109/tcst.2016.2535260>
- [8] Muhammad, M., Abdullahi, A. M., Bature, A. A., Buyamin, S., Bello, M. "LMI-based Control of a Double Pendulum Crane", *Applications of Modelling and Simulation*, 2(2), pp. 41–50, 2018. [online] Available at: [https://www.researchgate.net/publication/329100473\\_LMI-Based\\_Control\\_of\\_a\\_Double\\_Pendulum\\_Crane](https://www.researchgate.net/publication/329100473_LMI-Based_Control_of_a_Double_Pendulum_Crane) [Accessed: 26 June 2023]
- [9] Kiss, B., Lévine, J., Mullhaupt, P. "Modelling, Flatness and Simulation of a Class of Cranes", *Periodica Polytechnica Electrical Engineering*, 43(3), pp. 215–225, 1999. [online] Available at: <https://pp.bme.hu/ee/article/view/1030> [Accessed: 26 June 2023]
- [10] Levine, J. "Analysis and control of nonlinear systems: A flatness-based approach", Springer, 2009. ISBN 978-3-642-00838-2 <https://doi.org/10.1007/978-3-642-00839-9>
- [11] Boustany, F., d'Andrea Novel, B. "Adaptive control of an overhead crane using dynamic feedback linearization and estimation design", In: *Proceedings 1992 IEEE International Conference on Robotics and Automation*, Nice, France, 1992, pp. 1963–1964. ISBN 0818627204 <https://doi.org/10.1109/robot.1992.219942>
- [12] Sira-Ramírez, H. "Sliding Mode Control: The Delta-Sigma Modulation Approach", Birkhäuser Cham, 2015. ISBN 978-3-319-17256-9 <https://doi.org/10.1007/978-3-319-17257-6>
- [13] Lee, L. H., Huang, P. H., Shih, Y. C., Chiang, T. C., Chang, C. Y. "Parallel neural network combined with sliding mode control in overhead crane control system", *Journal of Vibration and Control*, 20(5), pp. 749–760, 2014. <https://doi.org/10.1177/1077546312464681>
- [14] Kim, G. H., Hong, K. S. "Adaptive Sliding-Mode Control of an Offshore Container Crane With Unknown Disturbances", *IEEE/ASME Transactions on Mechatronics*, 24(6), pp. 2850–2861, 2019. <https://doi.org/10.1109/tmech.2019.2946083>
- [15] Xing, X., Liu, J. "State-estimator-based robust vibration control of crane bridge system with trolley via PDE model", *Communications in Nonlinear Science and Numerical Simulation*, 99, 105799, 2021. <https://doi.org/10.1016/j.cnsns.2021.105799>
- [16] d'Andréa-Novel, B., Lévine, L. "Modelling and Nonlinear Control of an Overhead Crane", *Robust Control of Linear Systems and Nonlinear Control: Proceedings of the International Symposium MTNS-89, Volume II*, Amsterdam, Netherlands, 1990, pp. 523–529. ISBN 9780817634704 [https://doi.org/10.1007/978-1-4612-4484-4\\_52](https://doi.org/10.1007/978-1-4612-4484-4_52)
- [17] Isidori, A. "Elementary Theory of Nonlinear Feedback for Multi-Input Multi-Output Systems", In: *Nonlinear Control Systems*, Springer London, 1995, pp. 219–291, ISBN 978-3-540-19916-8 <https://doi.org/10.1007/978-1-84628-615-5>
- [18] The Mathworks Inc. "MATLAB (R2021a)", [computer program] Available at: [https://www.mathworks.com/products.html?tid=gn\\_ps](https://www.mathworks.com/products.html?tid=gn_ps) [Accessed: 05 September 2023]